

Carbon dioxide and energy flux measurements in four northern-boreal ecosystems at Pallas

Mika Aurela¹⁾, Annalea Lohila¹⁾, Juha-Pekka Tuovinen¹⁾, Juha Hatakka¹⁾,
Timo Penttilä²⁾ and Tuomas Laurila¹⁾

¹⁾ Finnish Meteorological Institute, Atmospheric Composition Research, P.O. Box 503, FI-00101 Helsinki, Finland

²⁾ Natural Resources Institute Finland (Luke), P.O. Box 18, FI-01301 Vantaa, Finland

Received 4 Aug. 2014, final version received 22 Apr. 2015, accepted 22 Apr. 2015

Aurela M., Lohila A., Tuovinen J.-P., Hatakka J., Penttilä T. & Laurila T. 2015: Carbon dioxide and energy flux measurements in four northern-boreal ecosystems at Pallas. *Boreal Env. Res.* 20: 455–473.

The fluxes of carbon dioxide and energy were measured by the eddy covariance method for four contrasting ecosystems within the Pallas area in northern Finland: Kenttäröva spruce forest, open Lompolojänkkä wetland, treeless top of Sammaltunturi fell, and Pallasjärvi which is a lake. Clear differences in carbon and energy exchange were found among these ecosystems, in both the instantaneous fluxes and the related longer-term balances. The available solar energy and its partitioning into sensible and latent heat fluxes differed markedly among the sites. The characteristics of the CO₂ exchange at individual sites varied in terms of the maximum uptake and emission capacity and the associated responses to environmental drivers. The highest instantaneous fluxes were observed over wetland and forest. The mean annual balance showed a considerable net uptake at the wetland, while the balances of the fell top and the forest were both close to zero. The lake, on the other hand, was estimated to be a relatively large source of carbon dioxide. An upscaling exercise based on the actual land-use map of the surroundings demonstrated the importance of including all the major ecosystems in the landscape CO₂ balance.

Introduction

Climate warming is predicted to be especially intense at northern high latitudes (IPCC 2013). While the increase in the atmospheric carbon dioxide (CO₂) and methane (CH₄) concentrations are the main contributors to warming, the changing climate will have a feedback effect on the carbon cycling within the atmosphere-biosphere continuum. Warmer conditions during the growing season will increase gross primary productivity, but at the same time they enhance the decomposition of the vast carbon reservoir

present in the northern soils (Gorham 1991). At high northern latitudes, where the growing season length is restricted by low temperatures and the snow cover, prolongation of the growing season may similarly affect the net annual CO₂ exchange either by increasing it due to the enhanced carbon sequestration during the extended plant activity period (Myneni *et al.* 1997, Richardson *et al.* 2010), or by decreasing it due to enhanced soil respiration, especially in autumn (Piao *et al.* 2008, Vesala *et al.* 2010). Overall, the ecosystem functions are tightly coupled with the availability of solar energy and its

partitioning into sensible and latent heat fluxes, necessitating integrated measurements of atmosphere–ecosystem exchange to disentangle the various biogeochemical feedbacks involved in carbon cycling.

Ecosystem-scale CO₂ and energy flux measurements by the eddy covariance (EC) method became common during recent decades, and data for various ecosystems are available from different European (CarboEuropeIP, ICOS) and global (Ameriflux, Asiaflux, Fluxnet) networks (Baldochi 2003). However, there is a scarcity of integrated multi-site measurements for fragmented landscapes consisting of different ecosystem types. For a comprehensive landscape-scale CO₂ budget, for example, one needs to assess the atmosphere–ecosystem exchange for all the major ecosystems within the area in question. The instantaneous CO₂ exchange fluxes are controlled, on one hand, by meteorological variables, mainly the photosynthetic photon flux density (PPFD) and air temperature, which are similar over different ecosystems within the same area; on the other hand, exchange rates depend on ecosystem-specific variables, such as leaf area index (LAI) and soil temperature, humidity and carbon content, which may vary markedly between the ecosystems (Shaver *et al.* 2007, Owen *et al.* 2007, Kutch *et al.* 2009). The growing season length, which is an important determinant of the annual CO₂ balance, obviously depends on climatic features, but is also affected by local differences in temperature and energy fluxes resulting from the heterogeneity in physical vegetation characteristics (e.g. forest vs. open wetland). Albedo, in particular, may show large differences between adjacent ecosystems (Betts and Ball 1997, Eugster *et al.* 2000).

To improve the understanding of the landscape-scale carbon balances in the northern-boreal region, the Finnish Meteorological Institute has measured greenhouse gas and energy fluxes for more than a decade at Pallas in north-western Finland. There are currently four flux stations in operation within the same landscape, collectively referred to as the Pallas station. The surroundings of these flux stations include all the main ecosystems within the area: spruce forest, wetland, a treeless fell top, and a lake. In this paper, we focus on the EC measurements

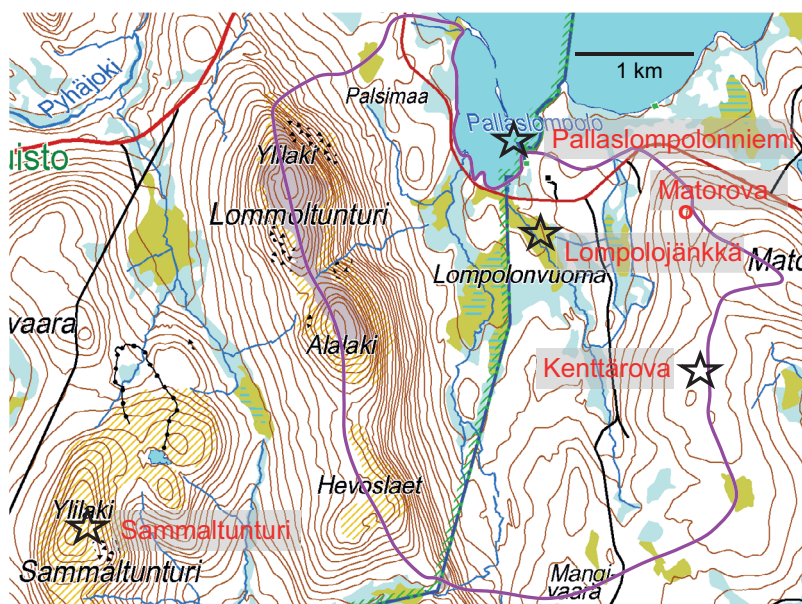
of CO₂ and energy fluxes conducted at these stations. We introduce the individual measurement sites and compare their characteristics, and then present an analysis of the CO₂ and energy exchange fluxes and their response to the main environmental drivers. Our objective was to study the variability in these fluxes in relation to the variability in the site characteristics within a heterogeneous landscape, and upscale the site-specific CO₂ flux data to obtain an estimate of the regional CO₂ balance. The more specific scientific questions addressed here are: (1) What controls the partitioning of the available energy into sensible and latent heat fluxes? (2) What explains the differences in the CO₂ exchange in summertime between different ecosystems? (3) What is the relative contribution of different ecosystems to the regional CO₂ balance?

Material and methods

Measurement sites

The Pallas station is situated close to the northernmost limit of the northern-boreal zone in an area comprising forests, wetlands, lakes and treeless fells. The mean annual temperature and the annual precipitation sum of -1.4 °C and 484 mm, respectively, were recorded by the nearest long-term weather station of Alamuonio (67°58'N, 23°41'E, 252 m a.s.l., 35 km from Pallas) for the period 1971–2000 (Drebs *et al.* 2002). The Pallas station has four separate EC flux measurement installations within 12 km of each other. Two of these sites are located within the Pallas-Yllästunturi National Park, and the other two are in the Finnish Forest Research Institute's research forests. The Pallaslompola catchment (Fig. 1) encompasses the treeless fell-tops and steep slopes of Lommoltunturi, spruce and pine forests on upland mineral soil, mesotrophic fen-type wetlands fed by the water from the surrounding uplands, and the inlet of a lake (Pallaslompola). These catchment ecosystems are covered by three flux measurement sites: (1) the Kenttäröva spruce forest, (2) the Lompola-jänkkä wetland, and (3) Pallaslompolonnemi at Pallasjärvi. The fourth flux measurement site lies on the treeless top of the Sammaltunturi fell.

Fig. 1. Map of the Pallas station area. The four flux measurement stations at Kenttäröva (Forest), Lompolojäykkä (Wetland), Sammaltunturi (Fell) and Pallaslompolonniemi (Lake) are indicated with stars. The lilac line denotes the Pallaslompolo sub-catchment, which is part of the Pallasjärvi catchment. The circle denotes the Matorova meteorological station. The Laukukero meteorological station is situated 10.6 km northwest of the Lompolojäykkä station. (The map is from the National Land Survey of Finland Database 12/2014).



We also used the data from two meteorological stations: Laukukero (fell) and Matorova (forest).

Kenttäröva spruce forest

The Kenttäröva site lies at an elevation of 347 m a.s.l. on a hill-top plateau, ca. 60 m above the surrounding plains (Fig. 1 and Table 1). A 20-m high measurement tower is situated in a Norway spruce forest (*Hylocomium-Myrtillus* type,

HMT) (Fig. 2a). In 2011, the mean stand density was 643 and 68 live stems per hectare for spruce and deciduous trees (mainly *Betula pubescens* (pubescent birch), some *Populus tremula* and *Salix caprea*), respectively. The dominant tree height was 14.5 and 10.3 m, and standing stem volume 71 and 8 m³ ha⁻¹ for spruce and deciduous trees, respectively. The age of the trees varied from 80 to 240 years. Among individual spruce trees the height varied greatly according to tree age, while the birches had a more even

Table 1. The instrumentation and characteristics of the flux measurement sites within the Pallas area.

	Wetland	Forest	Fell	Lake
Name of the station	Lompolojäykkä	Kenttäröva	Sammaltunturi	Pallasjärvi
Coordinates	67°59.835' N 24°12.546' E	67°59.237' N 24°14.579' E	67°58.400' N 24°06.939' E	68°0.280' N 24°12.254' E
Altitude (m a.s.l.)	269	347	565	267
Ecosystem	Mesotrophic fen	Spruce forest	Alpine tundra	Lake
Dominant vegetation	Sedges, shrubs	Norway spruce	Shrubs	n.a.
LAI (one-sided)	1.3	2.1	0.5	n.a.
Vegetation height (m)	0.4	13	0.2	n.a.
Soil type	Peat	Podzol	Bare bedrock, thin humus layer	n.a.
Measurements started in	April 2005	January 2003	June 2011	July 2013
Sonic anemometer	USA-1 (METEK)	USA-1 (METEK)	USA-1 (METEK)	USA-1 (METEK)
CO ₂ /H ₂ O analyzer	LI-7000 (Li-Cor)	LI-7000 (Li-Cor)	LI-7000 (Li-Cor)	LI-7000 (Li-Cor)
Measurement height (m)	3	23	2.5	2.5
Inlet-tube length (m)	9	8	25	10

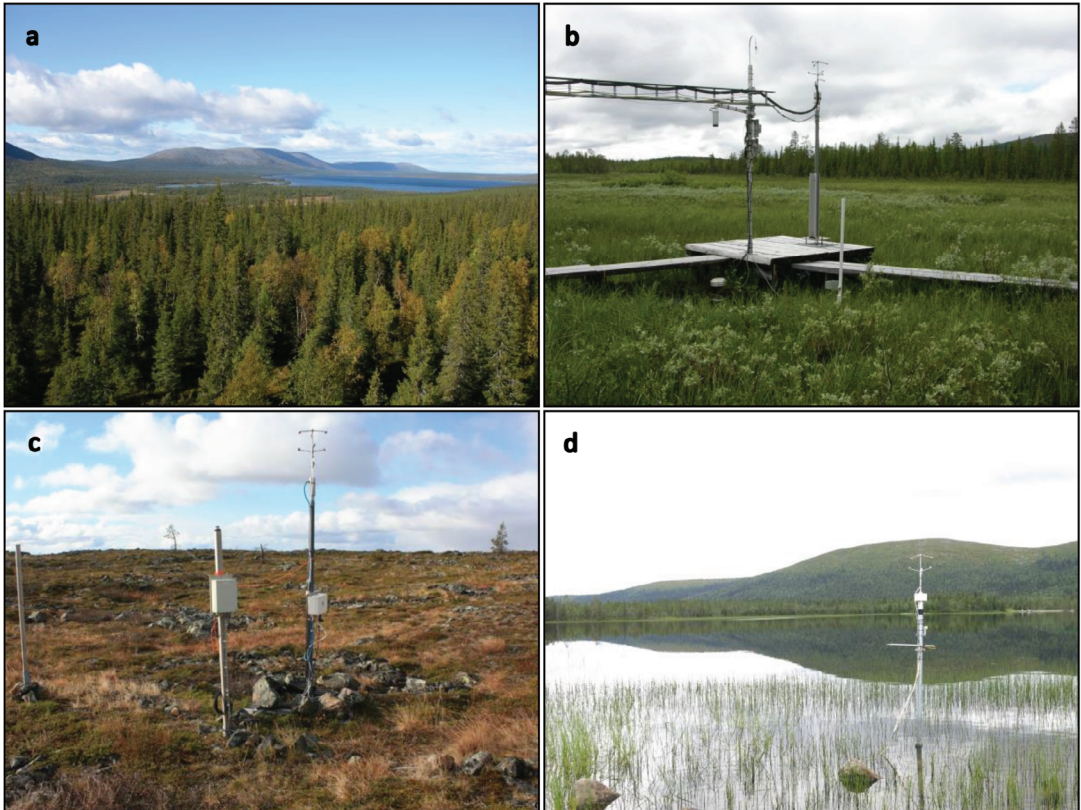


Fig. 2. Photographs of the flux measurement stations: (a) Forest (Kenttäröva), (b) Wetland (Lompolojänkki), (c) Fell (Sammaltunturi) and (d) Lake (Pallaslompolonniemi).

height distribution. Typically for north-boreal spruce stands, live canopies cover almost the entire length of the tree stems. The stand is regenerated naturally, but some forest management took place in the late 1960s, when most of the pubescent birch was harvested. A one-sided (i.e. half of total) LAI of 2.0 and $0.1 \text{ m}^2 \text{ m}^{-2}$ was estimated for the Norway spruce and pubescent birch trees, respectively, using tree diameter data and allometric functions (Marklund 1988). The main species of the ground floor are *Vaccinium myrtillus*, *Empetrum nigrum*, *Vaccinium vitis-idaea* and the forest mosses *Pleurozium schreberi*, *Hylocomium splendens*, and *Dicranum polysetum*. The soil type at the site is podzolic till. The snow cover maximum in Finland has often been observed at the Kenttäröva Forest site, with an average annual maximum value of 104 cm (81–125 cm) in 2008–2014. This site is hereafter referred to as ‘Forest’.

Lompolojänkki wetland

The Lompolojänkki site is located on an open, mesotrophic sedge fen (Figs. 1 and 2b, Table 1). The fen is characterized by a relatively high water level, almost the entire peat profile being water-saturated throughout the year. The field-layer vegetation in the wetter parts is dominated by sedges, with *Carex rostrata* as the most abundant species, accompanied by *C. chordorrhiza*, *C. magellanica* and *C. lasiocarpa*. *Menyanthes trifoliata* and *Equisetum fluviatile* are the most common herbs. Drier parts are characterized by fairly dense stands of *Betula nana*, with patches of *Salix lapponum* that also occur on the stream margins. Low shrubs, mainly *Andromeda polyfolia* and *Vaccinium oxycoccos*, can be found all over the fen, although with fairly low coverages. Due to the high water level, the moss layer is discontinuous (57% coverage of the total fen

area). *Sphagnum* species such as *S. riparium*, *S. fallax*, *S. jensenii*, and *S. teres* are abundant in the wetter surfaces, while *S. russowii* and *S. angustifolium* can be found on the ridges and low hummocks. Some brown moss species (*Warnstorfia exannulata*, *Helodium blandowii*, *Paludella squarrosa*) can also be found, but their coverages are very low.

The midsummer mean vegetation height on the fen is 40 cm, and a one-sided LAI of 1.3 m² m⁻² was measured at the height of summer in 2006 by a manual method (SunScan Canopy Analysis System SS1, Delta-T Devices). The peat depth is up to 2.5 m at the centre of the fen, in which peat accumulation started approximately 10 ky ago (Mathijssen *et al.* 2014); an average pH value of 5.5 was measured in the top peat layer, while the pH in the mire surface water varied from 5.5 to 6.5. The fen lies in a valley and is bounded by a forest that restricts the EC measurements in north-easterly and south-westerly wind directions. The prevailing wind directions, however, are those along the valley, i.e. south-easterly and north-westerly (Fig. 3a). For a more detailed description of Lompolojänkkä, see Aurela *et al.* (2009) and Lohila *et al.* (2010). This site is hereafter referred to as ‘Wetland’.

Sammaltunturi fell top

The Sammaltunturi site is on the top of a fell at an elevation of 565 m a.s.l., 100 m above the tree line (Figs. 1 and 2c, Table 1). Due to the craggy soil surface, the vegetation cover at Sammaltunturi site is discontinuous. Typically of the hemioarctic vegetation in this region, sporadic juniper bushes and low shrubs such as *Betula nana*, *Empetrum hermaphroditum*, *Vaccinium myrtillus*, *V. uliginosum*, *Arctostaphylos alpina*, and *Phyllodoce caerulea* characterize the field layer together with tussocks of some species (mostly *Festuca rubra*, *Juncus trifidus*) of the *Poaceae* family. Various species of lichens are abundant on the rocks and otherwise bare humus surfaces. The LAI of the ground vegetation has not been measured, but was visually estimated to be about 0.5 m² m⁻². The flux measurements are run in conjunction with the activities of the Global Atmosphere Watch station located on the

Sammaltunturi fell (Hatakka *et al.* 2003). This flux site is hereafter referred to as ‘Fell’.

Pallaslompolonniemi at Pallasjärvi

Pallasjärvi is a headwater lake with a surface area of 17.3 km² (Figs. 1 and 2d, Table 1). The Pallaslompolonniemi flux measurement site is situated on the tip of a small spit of land that is part of an esker gravel ridge, located partly beneath the lake surface. The ridge divides the area into a shallow and sheltered inlet (in wind directions of 180°–330°), which receives the surface waters from the Pallaslompolo catchment (Fig. 1), and a deeper lake (in directions 350°–50°). The data from other wind directions were discarded. The mean depth of the lake is about 1.5 and 5 m in the inlet and deeper parts, respectively. A more detailed description of Pallaslompolonniemi can be found in Lohila *et al.* (2015). This site is hereafter referred to as ‘Lake’.

Meteorological stations Laukukero and Matorova

The meteorological observations from the Laukukero and Matorova meteorological stations are presented here in order to illustrate the vertical gradients of temperature and wind speed and direction. Laukukero (68°3.770′N, 24°02.100′E, 760 m a.s.l) is one of the highest peaks in the chain of fells within the Pallas region. The treeless top of Laukukero is located 10.6 km north of Sammaltunturi. Matorova (67°59.999′N, 24°14.402′E, 340 m a.s.l.) is an air quality measurement station on a forested hill, located 1.4 km north of the Kenttäröva station (Fig. 1). This station is in the middle of a 1-ha plantation of young Scots pine trees.

Instrumentation

The same eddy covariance instrumentation for measuring the vertical exchange of CO₂ and sensible and latent heat was used at all four sites. The key instruments were the USA-1 (METEK) three-axis sonic anemometer/thermometer and

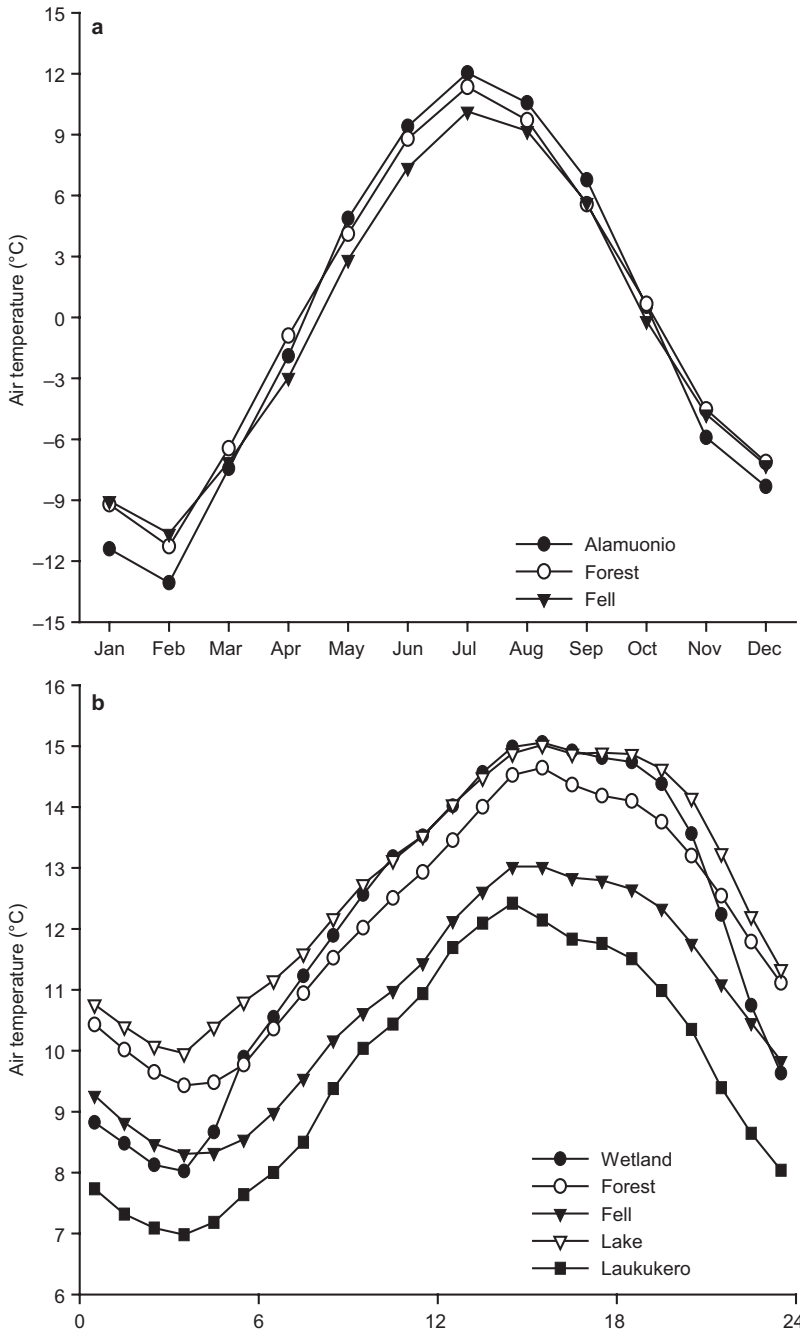


Fig. 3. (a) Monthly mean air temperatures at the Alamuonio meteorological station, Kenttäröva forest and Sammaltunturi fell top averaged for 2005–2013, and (b) mean diurnal cycle of air temperature at the flux measurement stations and the Laukukero meteorological station in July 2012

the closed-path LI-7000 (LI-COR Biosciences) CO₂/H₂O gas analyzer. The measurement heights and the lengths of the heated inlet tubes are given in Table 1. The mouth of the inlet tube was placed 10–15 cm below the sonic anemometer, and the flow rate in the tubes was normally 5–6 l min⁻¹. Synthetic air with a zero CO₂ con-

centration was used as the reference gas. The gas analyzers were calibrated typically every 3 months. For more details about the EC systems, see Aurela et al. (2009) and Lohila et al. (2015).

Supporting meteorological measurements were conducted at all flux sites, typically including air temperature and humidity, the soil tem-

perature profile, soil humidity or water-table depth and different radiation components (net radiation, incoming and reflected shortwave radiation, and PPFD). These instruments are detailed in Table 2. The Laukukero and Matorova stations are equipped with standard meteorological sensors (Table 3).

Data processing

Half-hourly fluxes were calculated using standard eddy covariance methods. The original 10-Hz EC data were block-averaged, and a double rotation of the coordinate system was performed (McMillen 1988). The time lag between the

Table 2. Instrumentation and measurement heights (m, relative to ground/water surface) of the supporting meteorological measurements at the four flux measurement sites within the Pallas area. These measurements are in addition to the standard meteorological observations in Table 3. In the case of multiple measurements at a given height, the number of sensors is given in parentheses. The different sensor models are given in brackets.

	Wetland	Forest	Fell	Lake
Air temp. (PT100, HMP series ¹ , Vaisala)	3	18	5	1.5
Air humidity (HMP series ¹ , Vaisala)	3	18	5	1.5
Soil temp. (PT100, IKES, Nokeval)	−0.05 (3), −0.07, −0.1 (2), −0.2 (2), −0.3 (3), −0.6	−0.05 (5), −0.1 (2), −0.2 (3), −0.5 (3)	−0.01, −0.1, −0.15, −0.2, −0.3	−0.2, −0.8
Soil humidity (ML2x, Theta probe)	−0.05, −0.07, −0.1	−0.05 (2), −0.2 (2)	−0.1	n.a.
Soil heat flux (HFP01–05, HukseFlux Thermal Sensors)	−0.07 (3)	−0.07 (2)	−0.15	n.a.
Short wave radiation (K&Z ²)	1.5 [CMP11]	22 [CMP21]	5 [CMP11]	n.a.
Upwelling SW radiation (K&Z)	1.5 [CMP11]	20 [CMP21]	n.a.	n.a.
Long wave radiation (K&Z)	n.a.	22 [CGR4]	n.a.	n.a.
Upwelling LW radiation (K&Z)	n.a.	20 [CGR4]	n.a.	n.a.
Photosynthetic photon flux density (PPFD) (K&Z, Li-Cor)	1.5 [LI-190SZ], 1.2 [PQS1] (2)	22 [PQS1], 1.2 [PQS1] (2)	2 [PQS1]	1.5 [PQS1]
Reflected PPF (K&Z, Li-Cor)	1.5 [LI-190SZ]	20 [PQS1]	n.a.	n.a.
Net radiation (K&Z)	1.5 [NR-Lite]	n.a.	n.a.	1.5 [NR-Lite]
Water Table Level (Campbell Scientific, Trafag)	[PDCR1830, 8438.66.2646]	n.a.	n.a.	[8438.66.2646]

¹) HMP45D, HMP33 or HMP155. ²) K&Z: Kipp&Zonen.

Table 3. Instrumentation and the measurement heights of meteorological measurements at the five stations within the Pallas area reporting synoptic messages to the observation network of the Finnish Meteorological Institute. The start year refers to the year when the station began transferring synoptic messages to the network.

	Forest	Wetland	Fell	Laukukero	Matorova
Elevation (m)	347	270	565	760	340
Start year	2002	2013	1996	1996	1995
Air temperature (PT100, Pentronic)	2, 21	2	5	2	2
Air humidity (HMP series ¹ , Vaisala)	2, 21	2	5	2	2
Wind speed and direction (UA2D, Adolf Thies ² ; WAA252/WAV252, Vaisala ³)	23	13	7	12	12
Air pressure (PTB series ⁴ , Vaisala)	2	2	2	2	2
Snow depth (SR50-45H, Campbell Scientific)	1.5	n.a.	n.a.	n.a.	n.a.
Precipitation (Pluvio2 weighing gauge, OTT Messtechnik)	1.5	n.a.	n.a.	n.a.	n.a.

¹) HMP45D or HMP33. ²) sonic anemometer. ³) heated cup and vane. ⁴) PTB201A or PTB220.

anemometer and gas analyzer signals, resulting from the transport through the inlet tube, was taken into account in the calculation of the flux quantities by maximizing the absolute value of the covariance in question. Compensation for air density fluctuations related to the sensible heat flux is not necessary for the present system (Rannik *et al.* 1997), but the corresponding compensation related to the latent heat flux was made for the CO₂ and H₂O fluxes (Webb *et al.* 1980). Corrections for the systematic high-frequency flux loss owing to the imperfect properties and setup of the sensors (insufficient response time, sensor separation, damping of the signal in the tubing and averaging over the measurement paths) were carried out using transfer functions with empirically-determined time constants (Moore 1986, Laurila *et al.* 2005).

The data with wind directions from unsuitable sectors were first discarded from the further analysis. The data from periods of weak turbulence were removed using site- and season-dependent friction velocity (u_*) limits: from the Wetland, the Forest and the Fell we accepted the data if $u_* > 0.15 \text{ m s}^{-1}$, $u_* > 0.2\text{--}0.3 \text{ m s}^{-1}$ (depending on the season), and $u_* > 0.2 \text{ m s}^{-1}$, respectively. For the Forest, an additional condition, $u_* < 0.5\text{--}0.7 \text{ m s}^{-1}$, was set due to a strong response of CO₂ flux to u_* also at high wind speeds. At the Lake, no explicit u_* limits were used, but the data were screened based on a footprint analysis. After additional screening for instrument failures, flow non-stationarity and data outliers, the final data sets covered 24% to 37% of the total period at the sites. In addition to the unavoidable wind direction limitations, the relatively low data capture was due to the stringent quality assurance criteria applied and the extreme winter conditions at these northern sites.

CO₂ exchange response functions

The main meteorological drivers of CO₂ exchange are generally considered to be radiation (for gross photosynthesis, GP) and temperature (for respiration, R). In order to compare the response of fluxes to these drivers at the sites, general response functions were fitted to the CO₂ flux data.

For the PPFd response of GP, a commonly-used hyperbolic function was adopted (Lasslop *et al.* 2008):

$$\text{NEE} = \frac{\alpha \times \text{PPFD} \times \text{GP}_{\text{max}}}{\alpha \times \text{PPFD} + \text{GP}_{\text{max}}} + R, \quad (1)$$

where NEE is the net ecosystem CO₂ exchange (i.e., the measured CO₂ flux), GP_{max} is the gross photosynthesis rate in optimal light conditions and α is the initial slope of the NEE versus PPFd relationship.

The temperature response of the nighttime respiration was estimated by a modified Arrhenius function

$$R = R_0 \exp \left[E \left(\frac{1}{T_0} - \frac{1}{T_{\text{air}} + T_1} \right) \right], \quad (2)$$

where R_0 is the rate of ecosystem respiration at 10 °C, E is an activation-energy-related physiological parameter, T_{air} is the air temperature, $T_0 = 56.02 \text{ K}$ and $T_1 = 227.13 \text{ K}$ (Lloyd and Taylor 1994). Air temperature was used instead of soil temperature in order to avoid interpretation problems due to differences in soil temperature sensor depths.

At the three terrestrial stations, the NEE function (Eq. 1) was fitted to the data collected in July 2012. No measurements were available from the Lake for that period, so the data from July 2013 were used instead. The respiration function (Eq. 2) was fitted to all available year-round nighttime (PPFD < 20 $\mu\text{mol m}^{-2} \text{ s}^{-1}$) data at all sites (Forest: 2003–2013, Wetland: 2005–2010, Fell: 2011–2013, Lake: July–October in 2013).

Gap filling of the CO₂ exchange data

In order to calculate the annual CO₂ balances, full time series are needed, and thus the gaps in the EC flux time series must be filled. The missing fluxes during the snow-free period were modelled in three steps utilizing Eqs. 1 and 2 (e.g. Aurela *et al.* 2009). First, the parameter E was determined with 10–15-day time steps by fitting the respiration model (Eq. 2) to the nighttime data, and an average E was calculated from the values obtained. Second, the nighttime data were re-divided into weekly periods, and R_0 was

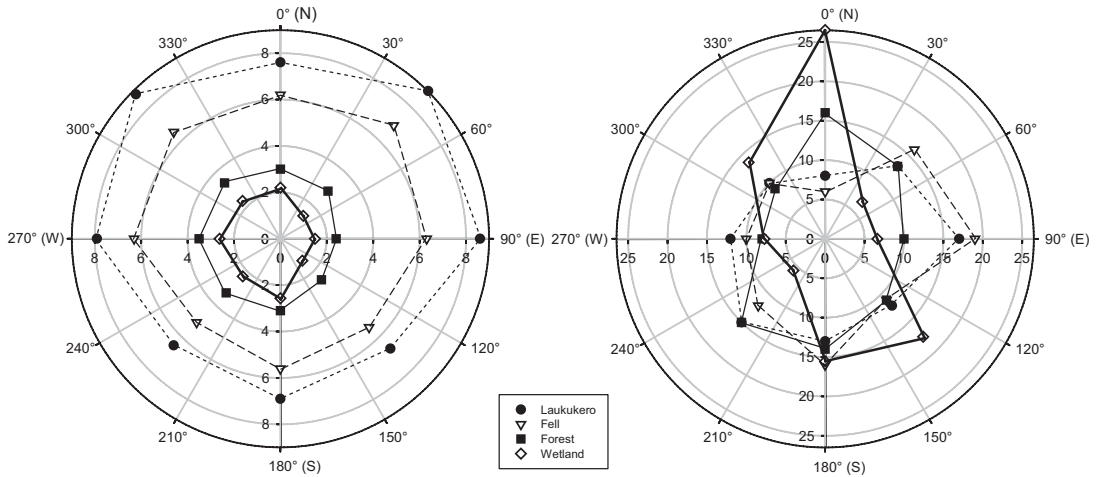


Fig. 4. (a) Average wind speeds (m s^{-1}) in different wind directions, and (b) relative wind direction frequencies (%) at different altitudes within the Pallas area: Wetland (Lompolojännkä, 269 m), Forest (Kenttäröva, 347 m), Fell (Sammaltunturi, 565 m) and the Laukukero meteorological station (760 m) in 2004–2013.

determined for each of these. Finally, using the same weekly division, the values of α and GP_{max} were obtained by fitting the NEE model (Eq. 1) to the full data set, also including the daytime data. In order to improve the time resolution of the GP parameterization, an additional multiplier (normalized phytomass index, PI) was introduced into Eq. 1; this procedure was described in detail by Aurela *et al.* (2001). Briefly, daily PI values were calculated from the difference between the daytime ($\text{PPFD} > 800 \mu\text{mol m}^{-2} \text{s}^{-1}$) and night-time ($\text{PPFD} < 20 \mu\text{mol m}^{-2} \text{s}^{-1}$) CO_2 fluxes and used as a multiplier of the first term on the right-hand side of Eq. 1. During winter with no CO_2 uptake, the data gaps were filled by a moving average with a varying (3–17 days) time window. At the Lake the data was gap filled by the monthly median values (Lohila *et al.* 2015).

Results and discussion

Meteorology

During 2003–2013, the mean annual temperatures were rather similar at the Fell, the Forest and the Alamuonio station (-0.5 , 0.4 and -0.1 °C, respectively), despite their differences in altitude. In the monthly mean tempera-

tures there was more variation among the sites (Fig. 3a), with the greatest annual amplitude (25 °C) being observed at the lowest site Alamuonio and the smallest amplitude (19 °C) at the Laukukero fell (760 m a.s.l.), highlighting the influence of site altitude. The diurnal temperature cycle showed the same pattern, with the greatest amplitude at the low-altitude Wetland site (Fig. 3b). There was a distinctive difference, however, between the Wetland and the nearby Lake located at the same altitude. Night temperatures were markedly higher at the Lake due to the large heat capacity of the waterbody.

Expectedly, the wind speeds were highest at Laukukero and got weaker with decreasing altitude (Fig. 4a). The mean wind speeds in July (in 2004–2012) were 7.8 , 6.0 , 2.9 and 2.1 m s^{-1} at Laukukero, the Fell, the Forest and the Wetland, respectively. The mean annual wind speeds at these sites were 9.5 , 7.0 , 2.9 and 2.2 m s^{-1} , respectively. The wind speeds at higher altitudes were distributed relatively evenly among different directions, with slightly higher speeds from the east and the west at the fell sites. At the low-altitude sites, especially at the Wetland, easterly winds are typically weaker. A clearer difference between the Wetland and Laukukero was observed in the wind direction distribution, with the Wetland showing a highly distinctive pattern dominated by southerly (S–SE) and northerly

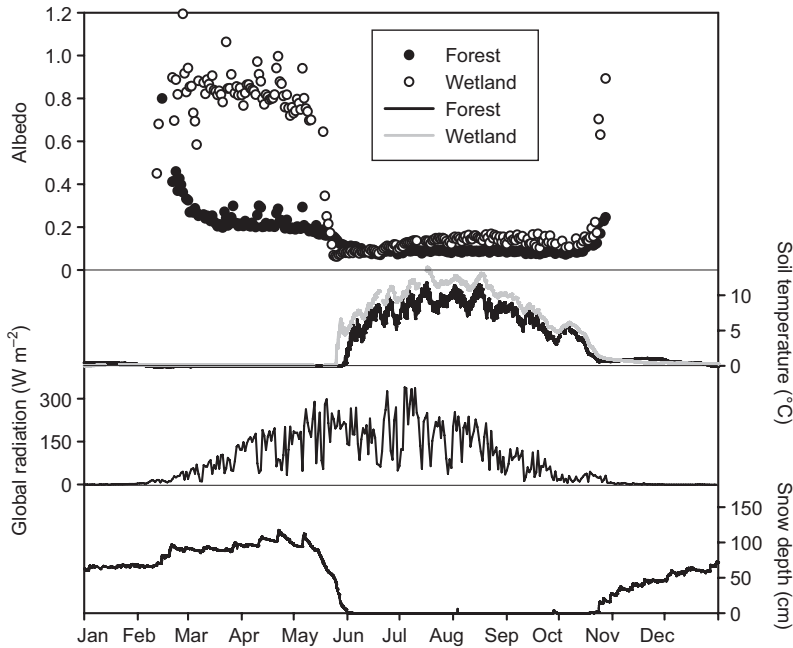


Fig. 5. Annual cycles of the midday albedo and soil temperature (at -5 cm) at the Forest and Wetland sites in 2012. The daily average global radiation and snow depth data are from the Forest site. The daily albedo values were averaged from the midday (10:00–14:00 local winter time) short-wave radiation ratio.

(N–NW) winds, while at higher altitudes these directions are among the most infrequent ones (Fig. 4b). This results from the topography of the area, which funnels the flow along the valley of the Lompolojännkä wetland (Fig. 1). In winter-time, south-westerly winds are more common within the Pallas region, as is typical for the whole of Finland (Drebs *et al.* 2002).

Energy fluxes

At these latitudes, i.e. north of the Arctic Circle, the summer is relatively short. The snow-free period at Pallas lasts for about five months, typically from mid-May to mid-October, as was the case at the Forest site in 2012 (Fig. 5). The presence of snow imposes marked restrictions upon the ecosystem functions, which are ultimately driven by the available solar energy. The incoming solar radiation is already at a relatively high level in April, but the persisting snow cover inhibits the utilisation of this energy. This is especially evident in treeless ecosystems such as wetlands. At the Wetland, the albedo remained high (> 0.8) until the snow was completely melted, while at the Forest the albedo was markedly lower (< 0.2) due to the

dark Norway spruce canopy (Fig. 5). Such a difference between forests and treeless ecosystems is typically observed during the snow-covered period (Betts and Ball 1997). The disappearance of the snow is clearly seen in the albedo of a wetland, which is typically reduced from 0.8 to 0.1 within a single week. Despite the lower forest albedo, the snow melts 1–2 weeks later at the Forest than at the Wetland due to the shading of the forest floor. At the Forest site, the snow melt day varied from 19 May to 1 June in 2006–2013.

A similar phase difference was observed in soil temperatures, which remained close to zero during the whole winter but increased quickly as soon as the snow melted (Fig. 5). The uppermost soil layers (-5 cm) were frozen during the winter months, but the soil temperature of deeper layers (below -20 cm) typically remained above zero during the whole winter.

The timing of the snow melt is a key question when considering the consequences of global warming at these latitudes (Aurela *et al.* 2004). With an earlier snow melt there would be a great potential for an earlier start to the growing season due to the availability of solar energy. In the autumn, the situation is different, as the incoming radiation is already highly limited at the time when the first snow typically appears

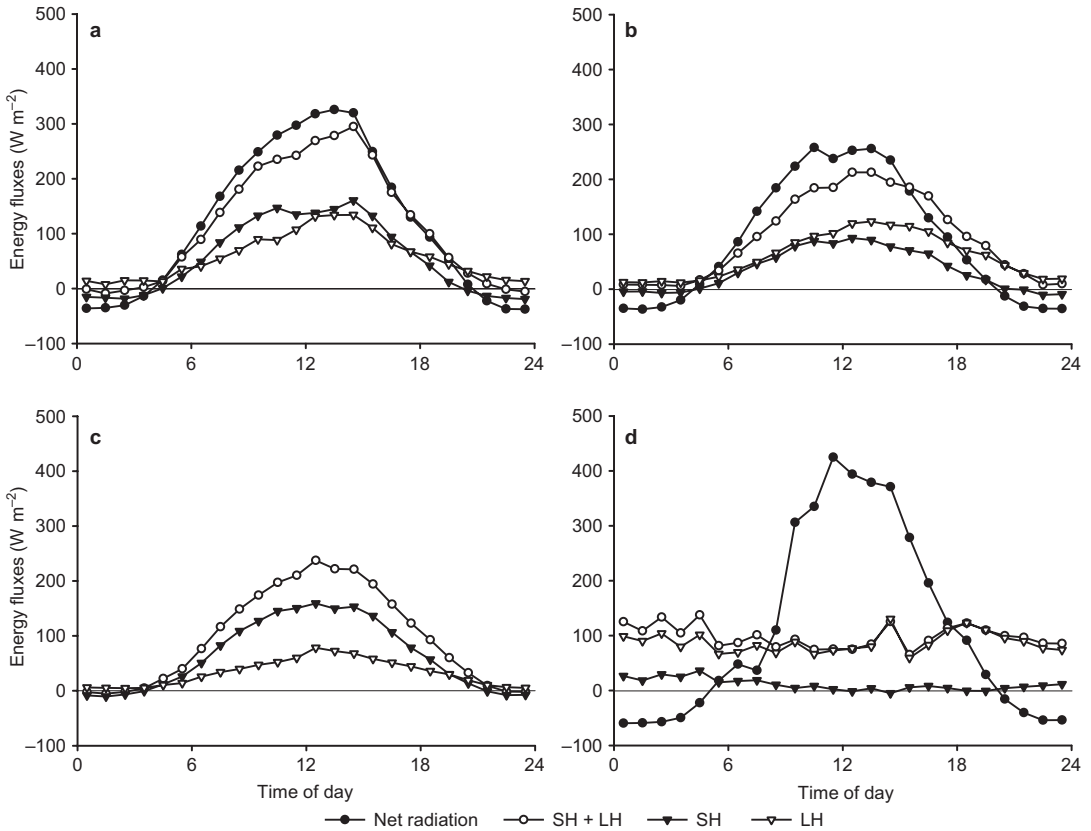


Fig. 6. Average diurnal cycles of net radiation, sensible heat (SH) and latent heat (LH) fluxes and their sum (SH + LH) at the four flux measurement stations in July 2012. (a) Forest, (b) Wetland, (c) Fell, and (d) Lake

(Fig. 5). Even if the first snow were to appear later owing to a warmer climate, the plants could not sustain growth any longer because of the lack of solar radiation.

After the snowmelt, when the ground is bare and dark, the albedo of wetlands reaches its annual minimum, thereafter starting to gradually increase as the plants emerge and grow (Aurela *et al.* 2002). No such pattern is observed in forests, where the albedo stays at approximately the same level during the whole course of the summer. The mean albedo in July 2012 was 0.13 and 0.09 at the Wetland and the Forest sites, respectively. These are typical values for coniferous forests and open wetlands in high northern latitudes in summer. Petzold and Rencz (1975) and Eugster *et al.* (2000) reported albedos of 0.11–0.18 and 0.05–0.11 for open wetlands and boreal/subarctic coniferous forests, respectively. The difference in albedo of these contrasting ecosystems was also

reflected in the net radiation (NR) observed at the flux sites at Pallas (Fig. 6): the mean midday net radiation in July 2012 was 320 W m^{-2} at the Forest and 250 W m^{-2} at the Wetland. The highest NR, about 400 W m^{-2} , was observed at the Lake. Albedo was not measured at the Lake, but previous observations indicate that the midday albedo of lakes at these latitudes is about 0.05–0.06 (Beyrich *et al.* 2006, Eugster *et al.* 2000), which is in accordance with the higher NR values.

In July, the main part of the available energy (i.e., net radiation) was transformed into the sensible heat (SH) and latent heat (LH) fluxes, when integrated over the diurnal cycle (Fig. 6). In daytime, part of the energy went into heating of the soil, water and canopy, if present. Part of that energy was subsequently released during the night as radiation (negative NR), LH and SH. In spring, the greatest part of the energy received in the daytime was not released during the fol-

lowing night but was stored by heating the soil and water bodies ($NR > LH + SH$). The seasonal heat storages were released in autumn ($NR < LH + SH$). In July 2012, the difference between NR and $SH + LH$ was relatively small: at the Wetland, the surface had already turned from a net sink to a net source of energy, while at the Lake and the Forest this switch took place in August. The highest difference between NR and $SH + LH$ in spring and autumn was observed at the Lake and the lowest at the Forest.

There was a very distinctive difference between the ecosystems in their SH/LH flux ratio (i.e. the Bowen ratio, β) in July. At the Fell, the SH flux was markedly greater than the LH flux, and the midday (11:00–13:00) β calculated from the mean diurnal cycle equalled 2.1. At the Forest, this ratio was 1.1, which is comparable to that of the spruce forest at Flakaliden, Sweden, where β varied between from 0.79 to 1.07 during three summers (Wilson *et al.* 2002). In a review of FLUXNET sites, β of coniferous forest averaged 1.07 but was typically 0.5–1.1 (Wilson *et al.* 2002).

At the Wetland, heat transfer was LH-dominated with $\beta = 0.78$. This is very close to β observed at other similar wetlands in Finland (Kaamanen, $\beta = 0.74$; Aurela *et al.* 2001) and Sweden (Degerö, $\beta = 0.86$; Peichl *et al.* 2013), but somewhat higher than those reported for other northern wetlands (Runkle *et al.* 2014, Eugster *et al.* 2000), probably due to differences in the water table level (Runkle *et al.* 2014).

At the Lake, the SH fluxes were very small during the daytime and β was close to zero (0.04). This is in accordance with the few observations available from northern lakes, which range from 0.02 to 0.2 (Eugster *et al.* 2000, Nordbo *et al.* 2011). The Lake differed from the other sites at Pallas in showing only limited diurnal cycles in the SH and LH fluxes (Fig. 6d; Lohila *et al.* 2015).

Based on an extensive review across different ecosystems, Eugster *et al.* (2000) suggested that the Bowen ratio is more sensitive to the vegetation type than to the climatological zone. Low β is often observed concurrently with high soil moisture and great photosynthetic capacity of vegetation (Wilson *et al.* 2002). Among the present study sites, β varied in a logical manner:

β was the lowest at the Lake; this was followed by the Wetland with a high soil water content and high photosynthetic capacity, and the Forest with a high photosynthetic capacity but drier soil; largest β was found for the Fell where the soil is dry and the photosynthetic capacity is relatively low.

CO₂ exchange

Similarly to the energy fluxes, the characteristics of CO₂ exchange differed markedly between the four ecosystems studied here. In July, the highest gross photosynthetic rates were observed at the Wetland, with somewhat lower values at the Forest (Fig. 7a). The maximum midday uptake period was a little later in the year at the Forest, where the diurnal cycles peaked in August (Fig. 8). A clear PPFD response was also observed at the Fell, while the GP_{max} of the Lake was expectedly close to zero. On average, the Lake is a consistent source of CO₂, but a weak diurnal cycle was observed also at this site during the summer months. This cycle can be partly attributed to the aquatic plants growing in the shallow parts of the lake (Lohila *et al.* 2015), but it is likely that also the surrounding terrains had some impact on the observed fluxes, especially during stable nighttime conditions. The respiration parameters indicate that the Wetland had the strongest temperature response, while the basal respiration (i.e., R at 10 °C) was highest at the Forest. The respiration rates at the Fell and the Lake followed the pattern evident in the GP_{max} values, with the smallest CO₂ fluxes being observed at the Lake (Fig. 7b).

The monthly-averaged diurnal cycles clearly illustrate the seasonal development of the CO₂ fluxes at different sites (Fig. 8). While in July the CO₂ uptake and respiration were highest at the Wetland, the situation was different during the other months. In August, a similar uptake rate was observed at the Wetland and the Forest, while during the other months with significant photosynthetic activity (from May to October) the midday uptake was higher at the Forest. The seasonal variation at the Fell was similar to that at the Forest; there was a clear diurnal cycle during six months, whereas at the Wetland the

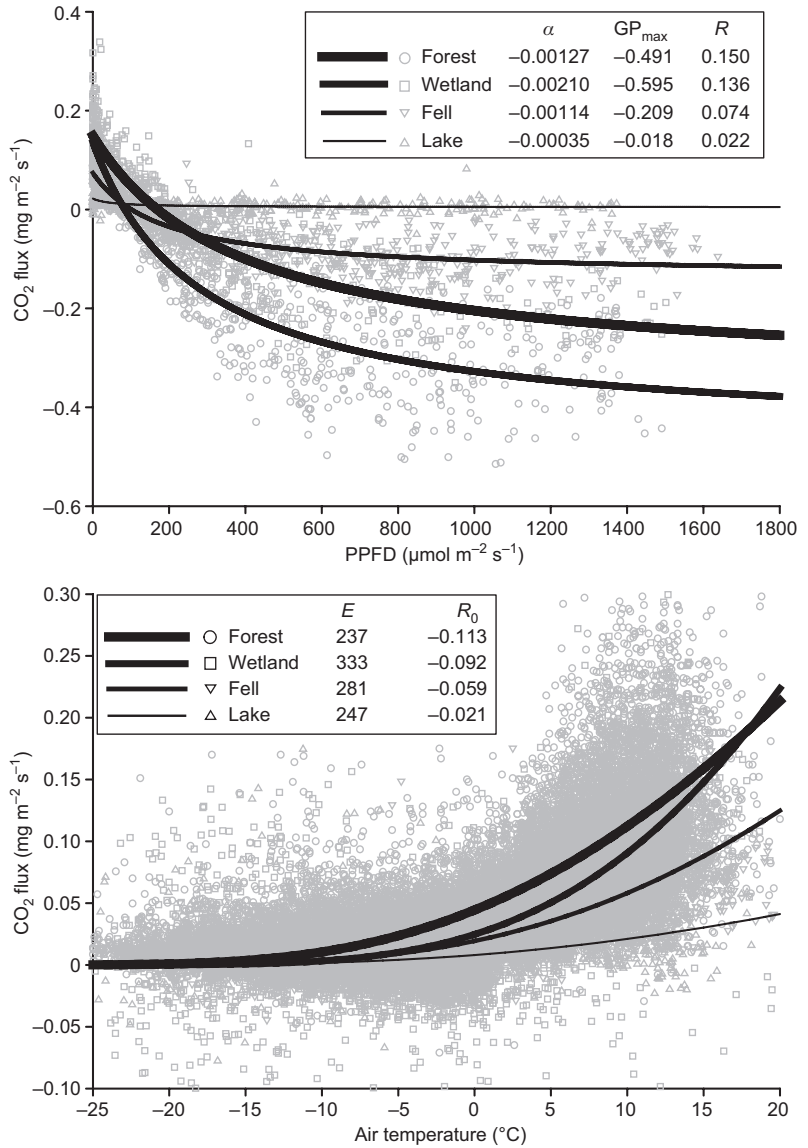


Fig. 7. (a) Radiation response of the net ecosystem CO₂ exchange (Eq. 1), and (b) the temperature response of the nighttime respiration (Eq. 2). The radiation response equation was fitted to the data of July 2012 at the Forest, Wetland and Fell sites and of July 2013 at the Lake site. The temperature response equation was fitted to the year-round data for all available years.

uptake period was shortened from both ends by a month. In the Lake data, the signal of photosynthesis is more discernible in these diurnal cycles than in the PPFD response curve. The wintertime efflux was clearly highest at the Forest. The difference between the Forest and the Wetland is partly explained by the higher deep soil temperature of the Forest and partly by the solid ice cover at the Wetland that inhibits the free transportation of the soil CO₂.

It has been shown that LAI is one of the key scaling parameters of GP in various north-

ern ecosystems (Lindroth *et al.* 2008, Mbufong *et al.* 2014). Our observations did not fully comply with this scaling, as GP was higher at the Wetland than at the Forest, despite the higher LAI of the latter. However, our data are in good accord with the larger set of ecosystem-specific data (Fig. 9). The non-linear response found between LAI and GP at PPFD = 1000 $\mu\text{mol m}^{-2} \text{s}^{-1}$ (= GP₁₀₀₀) may here be associated with the shading effect within ecosystems with a high LAI or a pronounced vertical structure. This shading of the lower parts of the forest canopy

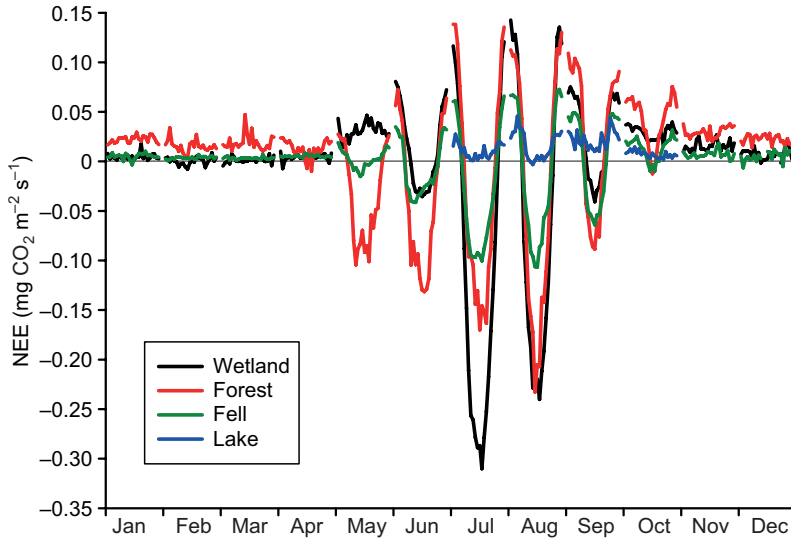


Fig. 8. Monthly mean diurnal cycles of net ecosystem CO_2 exchange in 2012 (Wetland, Forest, Fell) or in 2013 (Lake).

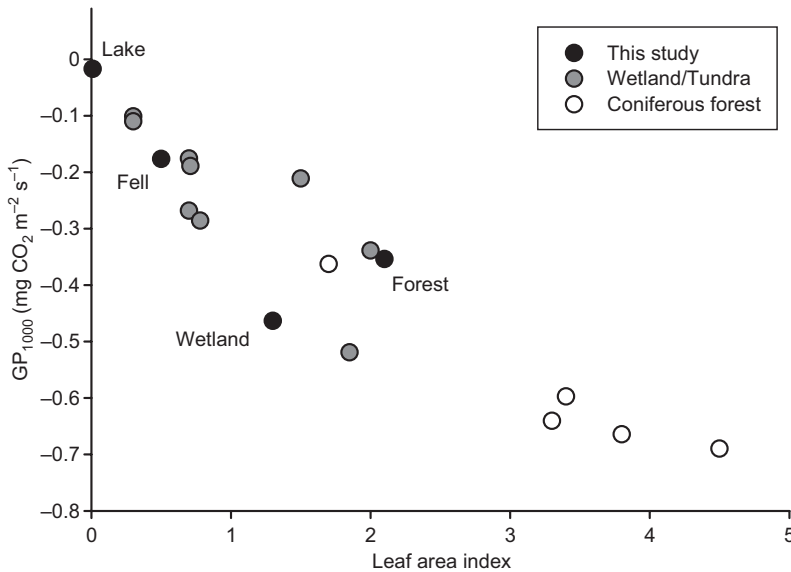


Fig. 9. GP_{1000} versus one-sided LAI during the peak growing season. GP_{1000} represents the gross photosynthesis at $\text{PPFD} = 1000 \mu\text{mol m}^{-2} \text{s}^{-1}$. This study: based on Eq. 1 with the parameters shown in Fig. 7a. Wetland/Tundra: data from northern wetlands and arctic tundra (Mbufong *et al.* 2014). Coniferous forest: data from European coniferous forests derived from Fig. 8 in Lindroth *et al.* (2008).

is one reason for the apparently inconsistent GP/LAI ratios between the Forest and the Wetland. The GP_{1000} at the Fell fits well into the pattern of tundra ecosystems with a low LAI (Fig. 9).

While the daytime uptake at the Forest was at its highest in August, the monthly net uptake already had its maximum in June, when the ecosystem respiration had not yet reached its higher summer level (Fig. 10). At the Wetland, the photosynthetic activity was so strong in July that, even though respiration was also maximal then, the corresponding monthly net balance showed the highest net uptake. The monthly bal-

ances at the Fell were in the same phase as those at the Wetland, with the highest sink observed in July. In August, the magnitude of the net CO_2 sink at the Fell was close to that observed at the Forest. The significance of the winter fluxes at the Forest is well manifested in these monthly CO_2 balances (Fig. 10).

The total wintertime (November–April) efflux at the Forest averaged over the 10 measurement years (2008 not included due to technical problems) was $290 \text{ g CO}_2 \text{ m}^{-2}$. This efflux was relatively stable, varying from 243 to $328 \text{ g CO}_2 \text{ m}^{-2}$. The annual net balance at the Forest

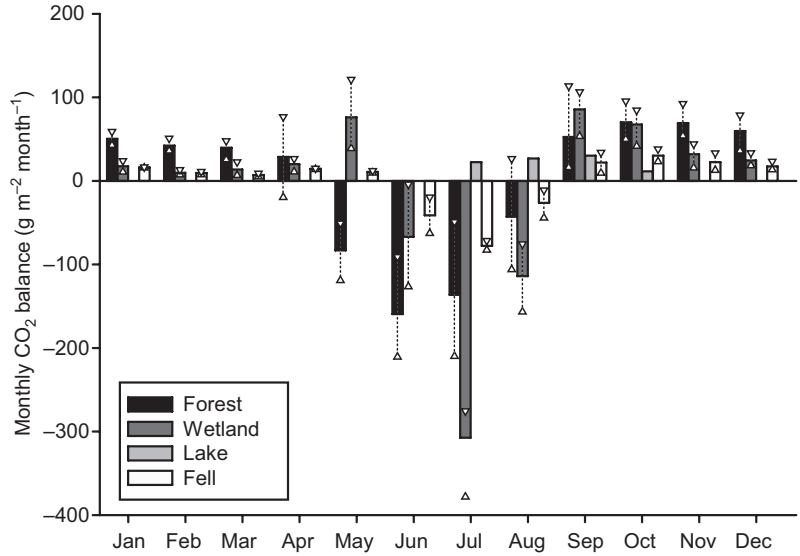


Fig. 10. Monthly CO₂ balances in 2012 (Wetland, Forest, Fell) or in 2013 (Lake). White triangles represent the interannual variation in the monthly balances at different sites (minimum and maximum).

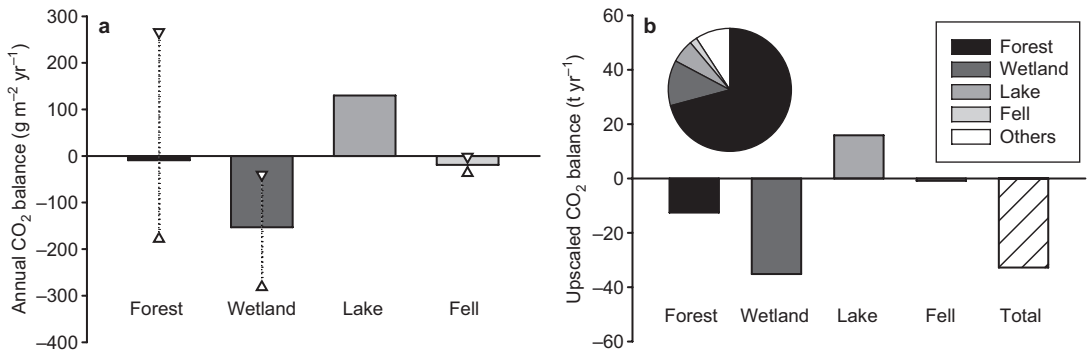


Fig. 11. (a) Annual CO₂ balances as a means of all available years (Forest 10 yr, Wetland 5 yr, Fell 2 yr and Lake 1 yr (based on 3 months)). White triangles represent the interannual variation at the site (minimum and maximum). (b) The pie-chart illustrates the relative area of different ecosystems within a 25-km radius around the Forest site (total 196 000 ha). The bars represent total upscaled CO₂ balances over that area.

was $-9 \text{ g CO}_2 \text{ m}^{-2}$ (uptake) (Fig. 11a), which does not differ from zero, when taking into account measurement uncertainties (cf. Aurela *et al.* 2009). The corresponding wintertime efflux at the Wetland was markedly lower, $117 \text{ g CO}_2 \text{ m}^{-2}$, averaged over the five years (2006–2010) included here. However, this efflux too has a major effect on the annual balance, which was $-153 \text{ g CO}_2 \text{ m}^{-2}$ on average. The net balance during the predominantly snow-free months (May–October) was similar at these two sites: -299 and $-259 \text{ g CO}_2 \text{ m}^{-2}$ at the Forest and the Wetland, respectively. The third upland site, i.e. the Fell, had an annual balance of $-19 \text{ g CO}_2 \text{ m}^{-2}$, averaged over two years of measurements. This

observation of a near-zero balance is plausible, as on the fell top there is only a limited organic soil layer that could be accumulating or releasing significant amounts of carbon. Of the ecosystems considered here, only the lake was a marked net source of CO₂ ($130 \text{ g m}^{-2} \text{ yr}^{-1}$). It must be noted, however, that this annual balance was estimated based on a 3-month measurement period that covered slightly more than half of the open-water season (Lohila *et al.* 2015).

The net CO₂ exchange of terrestrial ecosystems is the result of a sensitive balance between photosynthesis and ecosystem respiration, and under unfavourable conditions the ecosystem may turn into a source of CO₂ on an annual

timescale (Valentini *et al.* 2000). High-latitude forests in general show weaker CO₂ exchange rates than forests at lower latitudes, and their annual CO₂ balances are more commonly positive, indicating a CO₂ source to the atmosphere (Valentini *et al.* 2000, Luysaert *et al.* 2007). In the present study, the mean annual CO₂ uptake observed at the Forest site was close to zero (−9 g m^{−2} yr^{−1}) with an interannual variation ranging from a moderate CO₂ uptake (−178 g m^{−2} yr^{−1}) to a high CO₂ release (+266 g m^{−2} yr^{−1}). Taking into account the carbon accumulating in the growing trees, the annual NEE estimates suggest that in most years the soil at the Forest site is losing carbon. This conclusion was supported by soil flux measurements conducted with the chamber technique (T. Penttilä unpubl. data). The EC measurements in a Scots pine forest at Sodankylä, 125 km south-east of Pallas, showed CO₂ fluxes alternating between a sink and a source during the most recent decade, with a small positive mean annual balance (Aurela *et al.* 2013). Lindroth *et al.* (2008) reported annual CO₂ balances for three Swedish spruce forests (from −1115 to +308 g m^{−2} yr^{−1}) and, considering the biomass increment, concluded that the soil was losing carbon at all of the sites, possibly due to the especially warm summers during the measurement years of 2001–2002. On the other hand, a Scots pine forest at Värriö, also located in northern Finland, has consistently been an annual CO₂ sink (−440 to −510 g m^{−2} yr^{−1} in 2013–2014) (S. Dengel pers. comm.).

The mean annual balance of −153 g CO₂ m^{−2} yr^{−1} observed at the Wetland indicates a somewhat higher net uptake than that observed at the Kaamanen fen in northern Finland (−81 g CO₂ m^{−2} yr^{−1}) in 1997–2002 (Aurela *et al.* 2004). As compared with Kaamanen, the Lompolojänkka fen is relatively lush, which may explain its higher uptake capacity. Even higher uptake rates have been observed at mid-boreal fens: at Siikaneva (61°50'N, 24°12'E) and Degerö (64°11'N, 19°33'E), where the mean annual uptake was −188 g CO₂ m^{−2} yr^{−1} (Aurela *et al.* 2007) and −201 g CO₂ m^{−2} yr^{−1} (Sagerfors *et al.* 2008), respectively. The higher net uptake was mainly due to the longer growing season at these more southern sites, but it should be noted that the summertime peak uptake is actually higher at Lompolojänkka.

The available EC data on the annual CO₂ balances of northern lakes is limited (Lohila *et al.* 2015), but the relatively high efflux observed at the Lake site of this study is in accordance with the even higher annual mean efflux of 282 g CO₂ m^{−2} yr^{−1} observed at a lake in southern Finland (Huotari *et al.* 2011).

Upscaling the CO₂ exchange

To reflect the spatial scale of typical remote-sensing products and regional climate models, a land-cover survey was carried out within a circular area with a 25-km radius (1963 km²) centred at Kenttäröva. The four ecosystems included in this study cover 91% of this area (coniferous forest 71%, treeless wetland 12%, water surfaces 6% and treeless fell tops 2%) (Lohila *et al.* 2015) (Fig. 11b). For upscaling our site-specific flux data, we pooled coniferous forests on mineral (48%) and peat (23%) soils, assuming equal NEE fluxes for them. The remaining 9% of the area consists of mixed forests, constructed areas, agricultural fields and treeless mineral soil.

We estimated the regional CO₂ budget for this 1963 km² area by multiplying the annual balances determined for each of the four ecosystems by the area of the corresponding land-cover class (Fig. 11b). These upscaled balances showed similar features to the site-specific balances expressed as flux densities (g CO₂ m^{−2} yr^{−1}) (Fig. 11a) with the highest uptake on wetlands and the highest emission from lakes. The contribution of the forests appears greater in the upscaled balance due to the dominant proportion of forests within the area. The nominal importance of wetlands was increased by upscaling, while that of the lakes was decreased. The total regional balance (representing 91% of the upscaling area of 1963 km²) was −3401 kg CO₂ yr^{−1} (averaging on −19.0 g CO₂ m^{−2} yr^{−1}).

Due to the heterogeneity in the landscape patterns, one can expect different results for different spatial scales. For the 105 km² catchment area of Pallasjärvi (*see* Fig. 1a in Lohila *et al.* 2015), for example, the different areas of the four key ecosystems (coniferous forest 61%, open wetlands 5%, fells 13%, lakes 17%, total 97%) changed the upscaled CO₂ balance to +54

kg yr⁻¹ (5.3 g m⁻² yr⁻¹). Thus the smaller-scale regional balance indicates that this area is a net source of CO₂, owing to the relatively high lake area within the catchment.

While these upscaling calculations may be considered a preliminary exercise, they clearly demonstrate the importance of multi-site measurements to cover the main ecosystems within a heterogeneous landscape.

Conclusions

Long-term, ecosystem-scale measurements of CO₂ fluxes, and carbon balance estimates derived from these, are available for a wide range of ecosystems with a global coverage. The upscaling of these data to a regional-scale balance constitutes a challenge and may be difficult, even on smaller geographical scales, if the landscape is fragmented and consists of various, differing ecosystems. On catchment and landscape scales, a single flux measurement station is unlikely to provide spatially representative data.

This paper demonstrates the large heterogeneity in the CO₂ and energy fluxes within a small landscape area, which is manifested in both the instantaneous fluxes and the related longer-term balances observed at individual measurement sites. The characteristics of CO₂ exchange vary markedly among the key ecosystems within the Pallas area in terms of the maximum uptake and emission capacity, the amplitude and phase of the phenological cycle and the associated response to environmental drivers. The partitioning of the available solar energy into sensible and latent heat fluxes also differs considerably between the sites.

The data collected at the four flux sites at Pallas represent the dominant ecosystems (spruce forest, open wetland, treeless fell, lake) of the subarctic Pallasjärvi catchment as well as a larger landscape-scale area (~2000 km²). Upscaling of the site-specific CO₂ fluxes shows the importance of the predominant ecosystems as components of the regional CO₂ balance, thus motivating multi-site measurements. In combination with the ongoing measurements of fluvial carbon fluxes and atmospheric methane fluxes, the extensive multi-year data set introduced here

will provide an excellent opportunity for a further study, in which these site-specific data are upscaled to a representative estimate of a total catchment-scale carbon balance.

Acknowledgements: This work was supported by the Ministry of Transport and Communication through ICOS-Finland. The authors would like to thank Eveliina Pääkkölä, Ahti Ovaskainen and Päivi Pietikäinen for their contribution to the operation of the measurement sites.

References

- Aurela M., Laurila T. & Tuovinen J.-P. 2002. Annual CO₂ balance of a subarctic fen in northern Europe: Importance of the wintertime efflux. *J. Geophys. Res.* 107: 4607, doi:10.1029/2002JD002055.
- Aurela M., Laurila T. & Tuovinen J.-P. 2004. The timing of snow melt controls the annual CO₂ balance in a subarctic fen. *Geophys. Res. Lett.* 31, L16119, doi:10.1029/2004GL020315.
- Aurela M., Lohila A., Hatakka J., Tuovinen J.-P., Penttilä T., Pumpanen J., Mäkiranta P. & Laurila T. 2013. Long-term CO₂ exchange at ICOS supersite in northern Finland. *Geophys. Res. Abs.* 15, EGU2013-13006. [Available at <http://adsabs.harvard.edu/abs/2013EGUGA..1513006A>]
- Aurela M., Lohila A., Tuovinen J.-P., Hatakka J., Riutta T. & Laurila T. 2009. Carbon dioxide exchange on a northern boreal fen. *Boreal Env. Res.* 14: 699–710.
- Aurela M., Riutta T., Laurila T., Tuovinen J.-P., Vesala T., Tuittila E.-S., Rinne J., Haapanala S. & Laine J. 2007. CO₂ exchange of a sedge fen in southern Finland — the impact of a drought period. *Tellus* 59B: 826–837.
- Aurela M., Tuovinen J.-P. & Laurila T. 2001. Net CO₂ exchange of a subarctic mountain birch ecosystem. *Theor. Appl. Climatol.* 70: 135–148.
- Baldocchi D. 2003. Assessing the eddy covariance technique for evaluating carbon dioxide exchange rates of ecosystems: past, present and future. *Global Change Biol.* 9: 479–492.
- Betts A.K. & Ball J.H. 1997. Albedo over the boreal forest. *J. Geophys. Res.* 102(D24): 28901–28909.
- Beyrich F., Leps J.-P., Mauder M., Bange J., Foken T., Huneke S., Lohse H., Luedi A., Meijninger W.M.L., Mironov D., Weissensee U. & Zittel P. 2006. Area-averaged surface fluxes over the LITFASS region based on eddy-covariance measurements. *Boundary Layer Meteorol.* 121: 33–65.
- Drebs A., Nordlund A., Karlsson P., Helminen J. & Rissanen P. 2002. *Climatological statistics of Finland 1971–2000*. Climatic Statistics of Finland 2002:1, Finnish Meteorological Institute, Helsinki.
- Eugster W., Rouse W.R., Pielke R.A., McFadden J.P.Sr, Baldocchi D.D., Kittel T.G.F., Chapin F.III, Liston G.E., Vidale P.L., Vaganov E. & Chambers S. 2000. Land-atmosphere energy exchange in arctic tundra and boreal forest: available data and feedbacks to climate. *Global*

- Change Biol.* 6: 84–115.
- Gorham E. 1991. Northern peatlands: role in the carbon balance and probable responses to climatic warming. *Ecol. Appl.* 1: 182–195.
- Hatakka J., Aalto T., Aaltonen V., Aurela M., Hakola H., Kompulla M., Laurila T., Lihavainen H., Paatero J., Salminen K. & Viisanen Y. 2003. Overview of the atmospheric research activities and results at Pallas GAW station. *Boreal Env. Res.* 8: 365–383.
- Huotari J., Ojala A., Peltomaa E., Nordbo A., Launiainen S., Pumpanen J., Rasilo T., Hari P. & Vesala T. 2011. Long-term direct CO₂ flux measurements over a boreal lake: Five years of eddy covariance data. *Geophys. Res. Lett.* 38: L18401, doi:10.1029/2011GL048753.
- IPCC 2013. Annex I: Atlas of global and regional climate projections. In: Stocker T.F., Qin D., Plattner G.-K., Tignor M., Allen S.K., Boschung J., Nauels A., Xia Y., Bex V. & Midgley P.M. (eds.), *Climate change 2013: the physical science basis*, Contribution of Working Group I to the Fifth Assessment Report of the Intergovernmental Panel on Climate Change, Cambridge University Press, Cambridge–New York, pp. 1311–1393.
- Kutsch W., Bahn M. & Heinemeyer A. 2009. Soil carbon relations — an overview. In: Kutsch W., Bahn M. & Heinemeyer A. (eds.), *Soil carbon dynamics. An integrated methodology*, Cambridge University Press, Cambridge, UK, pp. 1–15.
- Lasslop G., Reichstein M., Kattge J. & Papale D. 2008. Influences of observation errors in eddy flux data on inverse model parameter estimation. *Biogeosciences* 5: 1311–1324.
- Laurila T., Tuovinen J.-P., Lohila A., Hatakka J., Aurela M., Thum T., Pihlatie M., Rinne J. & Vesala T. 2005. Measuring methane emissions from a landfill using a cost-effective micrometeorological method. *Geophys. Res. Lett.* 32: L19808, doi: 10.1029/2005GLO23462.
- Lindroth A., Lagergren F., Aurela M., Bjarnadottir B., Christensen T., Dellwik E., Grelle A., Ibrom A., Johansson T., Lankreijer H., Launiainen S., Laurila T., Mölder M., Nikinmaa E., Pilegaard K., Sigurdsson B.D. & Vesala T. 2008. Leaf area index is the principal scaling parameter for both gross photosynthesis and ecosystem respiration of Northern deciduous and coniferous forests. *Tellus* 60B: 129–142.
- Lloyd J. & Taylor J.A. 1994. On the temperature dependence of soil respiration. *Func. Ecol.* 8: 315–323.
- Lohila A., Aurela M., Hatakka J., Pihlatie M., Minkkinen K., Penttilä T. & Laurila T. 2010. Responses of N₂O fluxes to temperature, water table and N deposition in a northern boreal fen. *Eur. J. Soil Sci.* 61: 651–661.
- Lohila A., Tuovinen J.-P., Hatakka J., Aurela M., Vuorenmaa J., Haakana M. & Laurila T. 2015. Carbon dioxide and energy fluxes over a northern boreal lake. *Boreal Env. Res.* 20: 474–488.
- Luyssaert S., Inglisma I., Jung M., Richardson A.D., Reichstein M., Papale D., Piao S.L., Schulze E.-D., Wingate L., Matteucci G., Aragao L., Aubinet M., Beers C., Bernhofer C., Black K.G., Bonal D., Bonnefond J.M., Chambers J., Ciais P., Cook B., Davis K.J., Dolman A.J., Gielen B., Goulden M., Grace J., Granier A., Grelle A., Griffith T., Grünwald T., Guidolotti G., Hanson P.J., Harding R., Hollinger D.Y., Hutrya L.R., Kolari P., Kruijt B., Kutsch W., Lagergren F., Laurila T., Law B.E., Le Maire G., Lindroth A., Loustau D., Malhi Y., Mateus J., Migliavacca M., Misson L., Montagnani L., Moncrieff J., Moors E., Munger J.W., Nikinmaa E., Ollinger S.V., Pita G., Rebmann C., Rouspard O., Saigusa N., Sanz M.J., Seufert G., Sierra C., Smith M.-L., Tang J., Valentini R., Vesala T. & Janssens I.A. 2007. CO₂ balance of boreal, temperate, and tropical forests derived from a global database. *Global Change Biol.* 13: 2509–2537.
- Marklund L.G. 1988. *Biomass functions for pine, spruce and birch in Sweden*. Report 45, Department of Forest Survey, Swedish University of Agricultural Sciences, Umeå.
- Mathijssen P., Tuovinen J.-P., Lohila A., Aurela M., Juutinen S., Laurila T., Niemelä E., Tuittila E.-S. & Väiliranta M. 2014. Development, carbon accumulation and radiative forcing of a subarctic fen over the Holocene. *Holocene* 24: 1156–1166.
- Mbufong H.N., Lund M., Aurela M., Christensen T.R., Eugster W., Friborg T., Hansen B.U., Humphreys E.R., Jackowicz-Korczynski M., Kutzbach L., Lafleur P.M., Oechel, W.C., Parmentier F.J.W., Rasse D.P., Rocha A.V., Sachs T., van der Molen M.M. & Tamstorf M.P. 2014. Assessing the spatial variability in peak season CO₂ exchange characteristics across the Arctic tundra using a light response curve parameterization *Biogeosciences Discussions* 11: 6419–6460.
- McMillen R.T. 1988. An eddy correlation technique with extended applicability to non-simple terrain. *Boundary-Layer Meteorol.* 43: 231–245.
- Moore C.J. 1986. Frequency response corrections for eddy correlation systems. *Boundary-Layer Meteorol.* 37: 17–35.
- Myneni R.B., Keeling C.D., Tucker C.J., Asrar G. & Nemani R.R. 1997. Increased plant growth in the northern latitudes from 1981 to 1991. *Nature* 386: 698–702.
- Nordbo A., Launiainen S., Mammarella I., Leppäranta M., Huotari J., Ojala A. & Vesala T. 2011. Long-term energy flux measurements and energy balance over a small boreal lake using eddy covariance technique. *J. Geophys. Res.* 116: D02119, doi:10.1029/2010JD014542.
- Owen K.E., Tenhunen J., Reichstein M., Wang Q., Falge E., Geyer R., Xiao X., Stoy P., Ammann C., Arain A., Aubinet M., Aurela M., Bernhofer C., Chojnicki B. H., Granier A., Gruenwald T., Hadley J., Heinesch B., Hollinger D., Knohl A., Kutsch W., Lohila A., Meyers T., Moors E., Moureaux C., Pilegaard K., Saigusa N., Verma S., Vesala T. & Vogel C. 2007. Linking flux network measurements to continental scale simulations: ecosystem carbon dioxide exchange capacity under non-water-stressed conditions. *Global Change Biol.* 13: 734–760.
- Peichl M., Sagerfors J., Lindroth A., Buffam I., Grelle A., Klemmedtsson L., Laudon H. & Nilsson M.B. 2013. Energy exchange and water budget partitioning in a boreal minerogenic mire. *J. Geophys. Res. Biogeosci.* 118: 1–13.
- Petzold D.E. & Rencz A.N. 1975. The albedo of selected

- subarctic surfaces. *Arctic Alpine Res.* 7: 393–398.
- Piao S., Ciais P., Friedlingstein P., Peylin P., Reichstein M., Luyssaert S., Margolis H., Fang J., Barr A., Chen A., Grelle A., Hollinger D.Y., Laurila T., Lindroth A., Richardson A.D. & Vesala T. 2008. Net carbon dioxide losses of northern ecosystems in response to autumn warming. *Nature* 451: 49–53.
- Rannik Ü., Vesala T. & Keskinen R. 1997. On the damping of temperature fluctuations in a circular tube relevant to the eddy covariance measurement technique. *J. Geophys. Res.* 102: 12789–12794.
- Richardson A.D., Black T.A., Ciais P., Delbart N., Friedl M.A., Gobron N., Hollinger D.Y., Kutsch W.L., Longdoz B., Luyssaert S., Migliavacca M., Montagnani L., Munger J.W., Moors E., Piao S., Rebmann C., Reichstein M., Saigusa N., Tomelleri E., Vargas R. & Varlagin A. 2010. Influence of spring and autumn phenological transitions on forest ecosystem productivity. *Phil. Tran. R. Soc. B* 365: 3227–3246.
- Runkle B.R.K., Wille C., Gazovic M., Wilmking M. & Kutzbach L. 2014. The surface energy balance and its drivers in a boreal peatland fen of northwestern Russia. *J. Hydrol.* 511: 359–373.
- Sagerfors J., Lindroth A., Grelle A., Klemedtsson L., Weslien P. & Nilsson M. 2008. Annual CO₂ exchange between a nutrient-poor, minerotrophic, boreal mire and the atmosphere. *J. Geophys. Res.* 113: G01001, doi:10.1029/2006JG000306.
- Shaver G.R., Street L.E., Rastetter E.B., van Wijk M.T. & Williams M. 2007. Functional convergence in regulation of net CO₂ flux in heterogeneous tundra landscapes in Alaska and Sweden. *J. Ecol.* 95: 802–817.
- Valentini R., Matteucci G., Dolman A.J., Schulze E.-D., Rebmann C., Moors E.J., Granier A., Gross P., Jensen N.O., Pilegaard K., Lindroth A., Grelle A., Bernhofer C., Grünwald T., Aubinet M., Ceulemans R., Kowalski A.S., Vesala T., Rannik Ü., Berbigier P., Loustau D., Guomundsson J., Thorgeirsson H., Ibrom A., Morgenstern K., Clement R., Moncrieff J., Montagnani L., Minerbi S. & Jarvis P.G. 2000. Respiration as the main determinant of carbon balance in European forests. *Nature* 404: 861–865.
- Webb E.K., Pearman G.I. & Leuning R. 1980. Correction of flux measurements for density effects due to heat and water vapour transfer. *Q. J. R. Meteorol. Soc.* 106: 85–100.
- Vesala T., Launianen S., Kolari P., Pumpanen J., Sevanto S., Hari P., Nikinmaa E., Kaski P., Mannila H., Ukkonen E., Piao S.L. & Ciais P. 2010. Autumn temperature and carbon balance of a boreal Scots pine forest in southern Finland. *Biogeosciences* 7: 163–176.
- Wilson K.B., Baldocchi D., Aubinet M., Berbigier P., Bernhofer C., Dolman H., Falge E., Field C., Goldstein A., Granier A., Grelle A., Halldor T., Hollinger D., Katul G., Law B. E., Lindroth A., Meyers T., Moncrieff J., Monson R., Oechel W., Tenhunen J., Valentini R., Verma S., Vesala T. & Wofsy S. 2002. Energy partitioning between latent and sensible heat flux during the warm season at FLUXNET sites. *Water Resour. Res.* 38: 1294, doi:10.1029/2001WR000989.